American Journal of Pathology, Vol. 167, No. 2, August 2005

Neurobiology

Dense-Core Plaques in Tg2576 and PSAPP Mouse Models of Alzheimer's Disease Are Centered on Vessel Walls

Samir Kumar-Singh,* Daniel Pirici,* Eileen McGowan,† Sally Serneels,* Chantal Ceuterick,‡ John Hardy,§ Karen Duff,¶ Dennis Dickson,† and Christine Van Broeckhoven*

From the Department of Molecular Genetics, Flanders Interuniversity Institute for Biotechnology (VIB8), and the Laboratory of Electron Microscopy,‡ Institute Born Bunge and University of Antwerp, Antwerp, Belgium; the Departments of Neuroscience and Pathology,† Mayo Clinic, Jacksonville, Florida; the Laboratory of Neurogenetics,§ National Institute on Aging/ National Institutes of Health, Bethesda, Maryland; and the Center for Dementia Research,¶ Nathan S. Kline Institute, Orangeburg, New York*

Occurrence of amyloid β (Aβ) dense-core plaques in the brain is one of the chief hallmarks of Alzheimer's disease (AD). It is not yet clear what factors are responsible for the aggregation of Aβ in the formation of these plaques. Using Tg2576 and PSAPP mouse models that exhibit age-related development of amyloid plaques similar to that observed in AD, we showed that ≈95% of dense plaques in Tg2576 and ≈85% in PSAPP mice are centered on vessel walls or in the immediate perivascular regions. Stereoscopy and simulation studies focusing on smaller plaques suggested that vascular associations for both Tg2576 and PSAPP mice were dramatically higher than those encountered by chance alone. We further identified ultrastructural microvascular abnormalities occurring in association with dense plaques. Although occurrence of gross cerebral hemorrhage was infrequent, we identified considerable infiltration of the serum proteins immunoglobulin and albumin in association with dense plaques. Together with earlier evidence of vascular clearance of Aβ, our data suggest that perturbed vascular transport and/or perivascular enrichment of Aβ leads to the formation of vasocentric dense plaques in Tg2576 and PSAPP mouse models of AD. ***(Am J Pathol 2005, 167:527–543)***

Alzheimer's disease (AD) is characterized by progressive deposition of the amyloid β protein (Aβ) in brain regions responsible for memory and cognition. The chief constituents of Aβ plaques are the Aβ peptides, Aβ40 and Aβ42, and according to the proposed amyloid hypothesis, Aβ is the key pathogenic molecule in the causation of AD.[1] Accordingly, mutations causing autosomal-dominant forms of AD identified within the Aβ precursor protein (APP) or presenilin proteins (PS1 and PS2)[2] increase the production of total Aβ (Aβ40 and Aβ42) or Aβ42.[3] However, the precise mechanism by which Aβ is neurotoxic, or deposited in plaques, has not been, as yet, resolved.

A variety of Aβ plaques are described in AD that range from diffuse to highly compacted plaques, the latter often contain a dense amyloid core and stain with fibril-binding dyes such as thioflavin S (ThS).[4] Consistent with *in vitro* neurotoxic properties of fibrillar Aβ,[5] dense plaques are associated with neuronal loss and a significant amount of neuritic pathology in the form of dystrophic neurites with vesicular organelles, dense bodies, and paired helical filaments.[4] A third form of Aβ deposition is in the walls of small arteries and arterioles within the leptomeninges and cortex as a segmental or concentric amyloid deposit (cerebral amyloid angiopathy, CAA).[6,7] With the recognition of Aβ deposition in vessels, considerable efforts have been devoted to studying the relationship between vessels and parenchymal Aβ plaques.[7–16] However, to date only one such entity has been accepted as a bona fide but smaller version of parenchymal Aβ plaques called drusige Entartung der Hirnarterien und capillaren or dyshoric angiopathy.[7,17] These deposits involve smaller

Supported by the Special Research Fund of the University of Antwerp; the International Alzheimer Research Foundation; the Fund for Scientific Research Flanders; the Interuniversity Attraction Poles program P5/19 of the Belgian Federal Science Policy Office, Belgium; and APOPIS within the 6th framework program of the European Commission.

Accepted for publication April 26, 2005.

Address reprint requests to Dr. S. Kumar-Singh, M.D., Ph.D., Department of Molecular Genetics VIB8, Neurodegenerative Brain Diseases Research Group, Molecular Neuropathology Project, University of Antwerp, Universiteitsplein 1, B-2610 Antwerp, Belgium. E-mail: samir.kumarsingh@ua.ac.be.

cortical arterioles and capillaries, and amyloid fibrils extend from the vessel into the surrounding neuropil and are associated with dystrophic neurites.[18]

In a rare familial AD associated with the Flemish APP substitution (Ala 692 Gly),[19] we recently reported that almost all dense-core plaques from various brain regions enclosed vessels or were associated with vessel walls.[15] Remarkably, dyshoric angiopathy was not only observed for capillaries and small arterioles, but also medium-sized arterioles.[15] Findings such as these have also been reported in rare familial forms of AD.[20] Recently, transgenic mouse models have been developed that exhibit progressive age-related Aβ plaques and CAA similar to that observed in AD.[21–24] Specifically, the dense plaques closely resemble human pathology, with neuritic dystrophy and neuronal loss in the surrounding parenchyma.[25]

The aim of this study was to explore the anatomical relationship between vessels (or vascular Aβ) and dense plaques in transgenic AD mouse models. In addition, we explored changes in vascular densities and structural microvascular abnormalities described previously in AD.[13,26] Using two AD mouse models—Tg2576 (APP/Sw or $APP_{K670N/M671L}$; line Tg2576)[22] and bigenic PSAPP (APP/Sw X $PS1_{M146L}$; line 6.2)[23,27]—we showed that the majority of the dense plaques are centered on vessel walls. We also showed considerable structural microvascular damage and blood-brain barrier (BBB) abnormalities in the vicinity of dense plaques.

Materials and Methods

Transgenic Mice

A total of 16 brains from hemizygous Tg2576 (n = 10, $APP_{K670N/M671L}$)[22] and bigenic PSAPP (n = 6, Tg2576 X $PS1_{M146L}$ line 6.2)[23,27] mice were studied. Tg2576 mice comprised four males (15, 17, 24, and 25 months of age) and six females (10 months of age, n = 2; 13 months of age, n = 2; and 17 and 24 months of age, n = 1 each); and PSAPP mice were three males (5, 11, and 20 months of age) and three females (5 months of age, n = 1; and 11 months of age, n = 2). Tg2576 founder was made in Swiss Webster X C57BL6/DBA2 hybrid and subsequently backcrossed to C57BL6/SJL, Swiss Webster, or B5/SJL-Swiss Webster F1. PSAPP were chiefly in Swiss Webster/C57D2F1. Control nontransgenic mice in $C57BL6/D2AF_1$ were 12, 18, and 24 months of age (n = 2 each). Mice were euthanized by cervical dislocation, and either the right or both hemispheres were immersion-fixed in 10% neutral buffered formalin (Tg2576) or 4% buffered paraformaldehyde for 18 hours (PSAPP) and embedded in paraffin, oriented coronally or sagittally. One PSAPP mouse that died immediately before being euthanized was also included in this study. In addition, tissue was also prepared for electron microscopy (see further). All animal experiments were approved by the University of Antwerp ethics committee and conducted according to the guidelines of the University of Antwerp and the National Institutes of Health.

Immunohistochemistry and Image Acquisition for Aβ and Vessel Markers on Paraffin-Embedded Specimens

For Aβ immunohistochemistry, the following antibodies were used: biotinylated-4G8 (Aβ17-24; Signet, Dedham, MA); 6E10 (Aβ5-11, Signet); JRF/AβN/11 (Aβ1-7);[28] JRF/cAb40/10, R209, and FCA3340 (specific for Aβ40);[28] and, JRF/cAb42/12, R226, and FCA3542 (specific for Aβ42).[28] Different antibodies on serial sections gave consistent staining patterns for dense plaques, which were defined as dense circumscribed aggregates, chiefly composed of Aβ40, and larger than 5 μm in diameter with clear limiting margins. Dense plaques recognizable on immunohistochemistry were also ThS-positive (see further). Dense vascular deposits were rejected when Aβ was confined to the vessel walls. Dyshoric angiopathy in which Aβ deposition involves parenchyma was considered as dense plaques. Furthermore, based on high specificity and almost no background, biotinylated-4G8 with 70% formic acid pretreatment for 5 minutes at room temperature was used for plaque-vascular association studies.

Utility of a panel of antibodies and lectins was explored as markers of murine vasculature: *Ricinus communis* agglutinin (RCA) I; *Ulex europaeus* agglutinin (UEA) I; *Griffonia* (*Bandeiraea*) *simplicifolia* (GSL $I\text{-}B_4$) (Vector Laboratories, Peterborough, UK); anti-mouse collagen IV (Chemicon, Temecula, CA); human smooth muscle cell, SMA (DAKO, Glostrup, Denmark); and three anti-mouse CD31 (PharMingen, San Diego, CA; Chemicon; and Cymbus, Hants, UK). From these markers, GSL $I\text{-}B_4$ and collagen IV emerged as the most efficient murine vascular markers and were subsequently used in this study. However, the reactivity of GSL $I\text{-}B_4$ (as well as of other endothelial markers) was substantially reduced in areas of dense plaque deposition. On the other hand, collagen IV immunoreactivity although relatively stable in plaque-rich areas, did not recognize all small vessels. Hematoxylin and eosin (H&E) stain was invariably used in conjunction with immunostaining because it was useful in identifying degenerating microvessels. For some series, Verhoeff's-van Gieson elastica stain was also used with biotinylated-4G8 histochemistry.

All immunohistochemical procedures were performed as detailed elsewhere.[15] Briefly, double immunohistochemistry was performed using species-specific or IgG subtype-specific secondary antibodies, conjugated to biotin for an additional amplification step or directly to horseradish peroxidase, alkaline phosphatase, or galactosidase. For monoclonal anti-Aβ antibodies, mouse-on-mouse kit (DAKO Ark system) was used. Color was developed with 3′3′diaminobenzidine (Roche, Nutley, NJ), 3-amino-9-ethylcarbazole (Roche), 5-bromo-4-chloro-3-indolyl-phosphate/nitro blue tetrazolium solution (Roche), or 5-bromo-4-chloro-3-indolyl-D-galactopyranoside (X-gal, Roche). Sections were counterstained with hematoxylin.

For each specimen, 40 serial sections of 4 μm thickness were sliced for two to three such series, spaced

≈50 μm apart. Dense plaques were systematically sampled on 4 to 10 random fields (depending on the objective used, see below) from the rhinal, frontal, hindlimb motor, cingulate, occipital cortices, hippocampus, as well as thalamus. All plaques encountered in the 11th to 30th section (80 μm) of each series were followed serially. An additional 10 flanking sections (thus 40 μm further on each end) were used only to conclude the plaques already being analyzed. Those that could not be concluded were rejected. For two mice we studied the entire brain region. For this, all plaques appearing on coronal brain slices for a Tg2576–24m (n = 210 plaques) and sagittal slices for a PSAPP-5m (n = 258 plaques) were studied with the above strategy. Images were grabbed by a ×20 lens covering a field of 0.092 mm^2 and occasionally by a ×40 (0.023 mm^2), archived into Analysis (Soft Imaging System, Münster, Germany) with each plaque being assigned a unique identity, montaged, and studied serially. More than 350 montages were generated with ≈35 Gb of images.

Assessment of Vascular Density, Microhemorrhages, and Serum Protein Infiltration

For vascular density assessments, two mice each of 11- to 13-month-old nontransgenic, Tg2576, and PSAPP mice were analyzed with GSL I-B_4, collagen IV, and goat anti-mouse immunoglobulin (Ig; Southern Biotechnology Inc., Birmingham, AL). Three images were grabbed by a ×20 objective (0.092 mm^2) from three serial sections from five cortical (rhinal, frontal, hindlimb motor, cingulated, occipital), hippocampal, and thalamic regions and were analyzed by densitometry as described earlier.[29]

Sixteen Tg2576 and PSAPP mice grouped as young (≤3 months, n = 7), adult (15 to 20 months, n = 4), and old (24 to 25 months, n = 5) together with nontransgenic mice of 12, 18, and 24 months (n = 2 each) were investigated for fresh or late microvascular hemorrhage (by H&E and Pearls' Prussian blue, respectively) and for parenchymal serum protein infiltration (Ig and albumin immunostaining). For Ig staining, sections were treated with 1:50 biotinylated goat anti-mouse Ig (DAKO) overnight and detected by streptavidin-biotin-horseradish peroxidase and 3′3′diaminobenzidine. For albumin staining, utility of three polyclonal antibodies was tested: biotinylated rabbit anti-mouse albumin (Autogen Bioclear, Wilts, UK), goat anti-mouse albumin (Bethyl, Montgomery, TX) and rabbit anti-mouse albumin (ICN Pharmaceutical, Cincinnati, OH). Rabbit anti-mouse albumin (ICN) was further used and detected as described for Ig. Microhemorrhages and serum staining were semiquantitatively scored independently by two investigators as: 0 (no microhemorrhage or reactivity detected in the entire brain section), 1 (≤2), 2 (>2 to 10), or 3 (>10 such observations). A total of 10 such series spaced up to 40 sections apart were analyzed and the scores averaged.

Fluorescent Microscopy

For investigating total and fibrillar Aβ content and comparing the staining patterns of dense plaques, two adjacent sections from each mouse were studied by Aβ immunolabeling and ThS. The sections were first stained with 1% solution of ThS (Sigma-Aldrich, Bornem, Belgium) and imaged using a Zeiss Axioskop 50 fluorescent microscope (Carl Zeiss NV, Zaventem, Brussels) equipped with specific filter sets (excitation, 395 to 440 nm; emission, 515 to 565 nm) connected to a UNIX workstation with an analysis program (Applied Imaging System, San Jose, CA). The sections were thereafter differentiated in 70% ethanol and processed further for Aβ histochemistry as described in the earlier section. Image analysis for Aβ- and ThS-stained sections was performed as described previously.[29]

Co-localization of Ig or albumin with Aβ was performed on 16 Tg2576 and PSAPP mice. Three series of two consecutive sections sampled systematically as described above were double-labeled for Aβ (biotinylated-4G8 or a combination of R209/R226 antisera[28]) with either Ig or albumin. In parallel, similar series were also prepared for ThS with Ig or albumin staining for each mouse. Using Alexa 488- or Alexa 594-labeled anti-mouse, anti-rabbit, or streptavidin biotin (Molecular Probes, Leiden, The Netherlands) with specific combinations of excitation and emission filter sets, proportions of dense-plaques positively labeled for Ig or albumin were manually assessed.

Thin and Ultrathin Section Preparation and Immunogold Labeling

Frontal and posterior cortex as well as the hippocampus of three PSAPP (5 months, n = 2; and 11 months) and 20-month-old nontransgenic mice (n = 2) were fixed in 4% neutral buffered glutaraldehyde followed by 2% buffered osmium tetraoxide, embedded in araldite, and sectioned with a Reichert Jung microtome equipped with a section counter as described previously.[15] Approximately 250, 1-μm-thick sections were sliced serially for each block. Semithin sections were stained with metachromatic methylene blue. A few sections were also stained immunohistochemically for Aβ to confirm the tinctorial properties of methylene blue. For this, the epoxy resin was removed as described[30] and processed as described for paraffin-embedded tissue. For ultrastructural microscopy, 0.1-μm-ultrathin sections were collected on copper grids before the start (prethin) and at the end (postthin) of each semithin series. Sections were contrasted with routine uranyl acetate and lead citrate, and analyzed by a Philips CM10 electron microscope equipped with a goniometric coordinator as described previously.[15] For immunogold labeling, tissue was fixed in 4% paraformaldehyde and 0.01% glutaraldehyde and embedded in Unicryl (BB Int., Cardiff, UK). Sections were collected on formvar-coated nickel grids (Ted Pella Inc., Redding, CA) and labeling performed with a polyclonal Aβ

antibody (kind gift from Dr. Konrad Beyreuther, ZMBH, University Heidelberg, Germany (*http://www.zmbh.uni-heidelberg.de/Beyreuther/*)) using anti-rabbit linked with 10-nm gold particles (BB Int.).

Morphometry, Simulations, and Statistics

The following attributes were measured manually by a specific tool within the AnalySIS package for both thin (4 μm) and semithin (1 μm) section analysis: 1) the total plaque size in its largest dimension in any of the serial section; 2) size of the dense core(s); and, 3) total number and diameter of the associated vessels within 4 μm of dense plaque (vessel bifurcation was counted as two). The chance of encountering vessels was calculated as follows: for a given vascular density, minimum area (A_T) containing at most one vessel was calculated by dividing A_T by the mean vessel area in this region, A_V, which provided a probability of a given vessel to be in this unique position ($P_V = A_V/A_T$). Presuming A_V to be circular, the probability of a circular plaque with radius R_P that would either overlap or juxtapose the vessel within a circle of radius $R_P + R_V +$ 4 μm was calculated (see Figure 4D). Because the number of vessels far exceeds the number of dense plaques, only one plaque could occur at one time. The probability for both events happening together is $P = P_V * P_P$ and was deemed significant if <0.05. Simulations were performed by randomly pitching circles of diameters 10, 20, and 40 μm to mimic plaques of these sizes. Simulations pitching partly outside the measured field, and for transgenic mice, pitching on the plaques, were rejected. All statistical analysis was performed either on S-Plus (Splus; Insightful Co., Seattle, WA) or by SPSS (SPSS Inc., Chicago, IL) and has been addressed in relevant sections in Results. Multiple comparisons were adjusted according to Bonferroni's method.

Results

Stereological Estimation of Dense Plaque-Vascular Association in Tg2576 and PSAPP Mice

We used stereological techniques to study the relationship between dense plaques and vessels in 10 hemizygous Tg2576 and 6 PSAPP mice brains. We first confirmed that both Aβ-immunoreactive and ThS-positive plaque burden increased exponentially with age and Aβ reactivity was consistently more than the ThS-positive plaque burden for all age groups.[31,32] Importantly, dense plaques recognized on immunohistochemistry (see Materials and Methods for inclusion criteria) were also ThS-positive. We also confirmed that PSAPP mice exhibit almost approximately fivefold accelerated pathology compared to Tg2576[23,31](see Figure 2D). Two ages for Tg2576 (17 and 24 months, $n =$ 1 each) and one age for PSAPP mice (5 months, $n = 1$) were available for paired gender comparisons. Consistent with a greatly accelerated pathology shown for female APP and PSAPP mice,[33,34] 17-month-old Tg2576 and 5-month-old PSAPP females deposited almost twice immunohistochemically-stained and ThS-positive plaques, compared to males. However, no differences in plaque load were observed between 24-month-old male and female Tg2576 that paralleled a high degree of within-gender heterogeneity in plaque burden observed for comparable age groups. Finally, consistent with earlier mass spectrometry data,[31] we also showed that the dense plaques and CAA in Tg2576 and PSAPP mice were predominantly composed of Aβ40 (data not shown).

In the first analysis for vascular-association, 2076 dense plaques systematically sampled from neocortical and hippocampal regions and studied end-to-end on 4-μm serial sections from nine Tg2576 and five PSAPP mice revealed a 94.1% and 84.8% association with small- to medium-sized vessels (Figure 1). To observe the generality of this observation, we further studied the entire brain region of a 24-month-old Tg2576 female and a 5-month-old PSAPP female mouse. A positive association was evident in 95.7% plaques for Tg2576–24m ($n = 210$ plaques) and in 85.3% for PSAPP-5m mouse ($n = 258$ plaques). The Tg2576–24m and PSAPP-5m were matched for gender and amyloid burden.

Together, our unbiased and systematic analysis of 2544 dense plaques from 16 Tg2576 and PSAPP mice revealed two kinds of plaque-vascular relationships. In the first type, one or more central dense-cores originated directly from vessel walls. This constituted 70.5% of all dense plaques in Tg2576 and 66.2% in PSAPP. In some plaques, the involved vessel had a $>$50-μm lumen diameter (for instance, see Figure 1, y3). In the second type of vascular relationship, dense plaques originated from perivascular regions. In both types of vascular involvement, new dense cores involved vessels at the plaque periphery. Cumulatively, a small but statistically significant difference was observed in the proportions of positively associated plaques in Tg2576 (94.3%, $n = 1216$) and PSAPP mice (84.8%, $n = 1328$) (Pearson $\chi^2 = 58.5$, $P < 0.001$) (Figure 2). This difference was consistent among all brain regions analyzed (Pearson χ^2 test, $P < 0.01$). Some variation was also noticed between mice of the same genotype, but this was primarily insignificant except for one of the oldest PSAPP mice. No difference in the proportion of positively associated dense plaques was observed between genders. In addition to dense plaques, some diffuse plaques were also observed around vessels; however, the relationship of diffuse plaques to vessels was not consistent.

Partly based on the data that dense plaques up to 40 μm in diameter could not associate by chance (see further), from 10-month-old Tg2576 mice ($n = 2$), the earliest plaque depositing mice in this series, we further studied 101 plaques $\leq$20 μm in diameter (mean

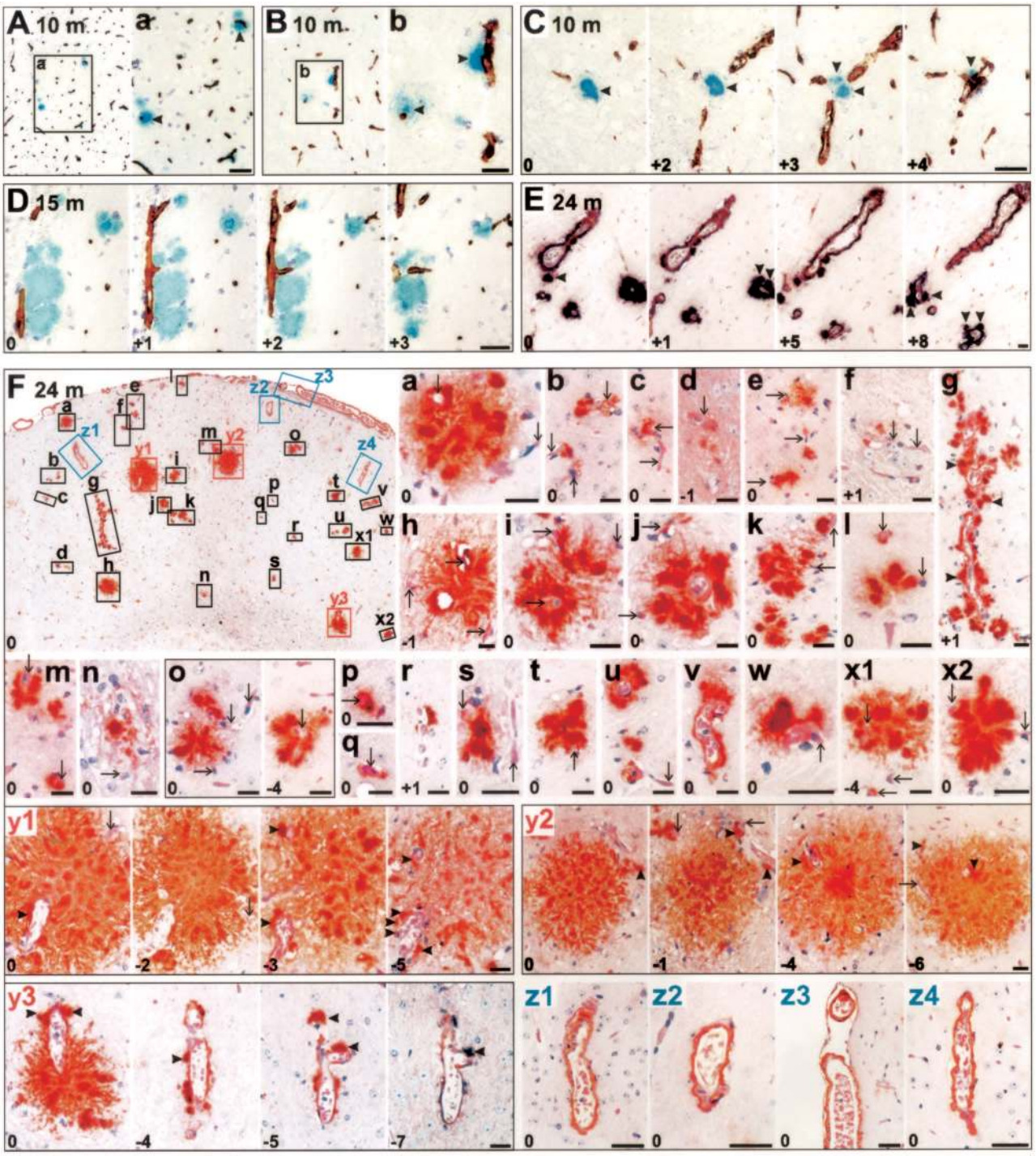

Figure 1. Vascular association of dense amyloid plaques in Tg2576 of different age groups studied on 4-μm serial sections. Integers on the **bottom left corner** represent relative sectional distance. **A–C:** Analysis of early dense plaques (**arrowheads**) from frontal neocortex of a 10-month-old Tg2576 mouse showing association with vessels [biotinylated Aβ antibody 4G8, blue; collagen IV (CIV), brown]. **D:** Hippocampus of a 15-month-old Tg2576 where linear streak of amyloid is deposited along vessels (Aβ, blue; CIV, brown). **E:** A thalamic region of a 24-month-old Tg2576 demonstrating development of small dense-core plaques (**arrowheads**) in association with vessels (Aβ, purple; GSL I-B_4, brown). Thalamus develops pathology very late in Tg2576 therefore these deposits represent early dense plaques. **F:** Frontal neocortical region of a 24-month-old female Tg2576 with **insets** numbered **a** through **z4** enlarged in the following micrographs shows that all dense Aβ deposits (**a** to **y3**) are either dense plaques (**arrowheads**) originating from vessel walls (**arrows**), or are classical CAA with Aβ limited to the vessel walls (**z1** to **z4**) (Aβ, brown; H&E counterstain; except section **y3** to **y4** where Aβ is purple and CIV is brown). Scale bars, 20 μm.

diameter, 13.8 μm; range, 5.52 to 19.95 μm; SD, 3.39 μm). Eighty-six percent of plaques were collected from the frontal cortex. With collagen IV alone that does not recognize all small capillaries, a positive association was evident in 81.2% of dense plaques. Because plaques larger than 20 μm were not analyzed from this series, this set of plaques was not considered for further stereology and statistical analyses.

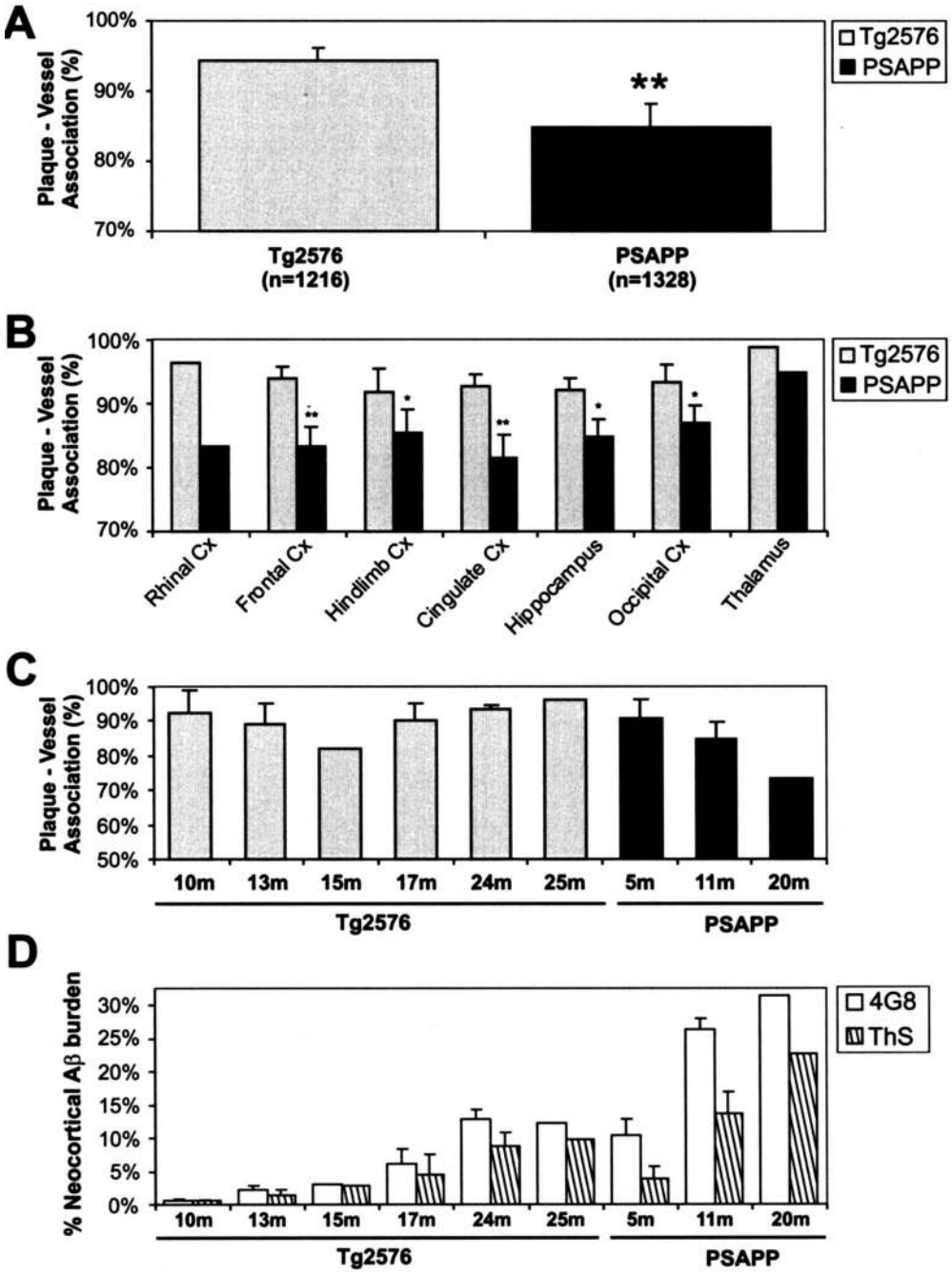

Figure 2. Vascular association of dense amyloid plaques in Tg2576 and PSAPP mice. **A–C:** Analysis for total plaques (**A**), for different brain regions (**B**), and for different age groups (**C**). **D:** Relative ThS and total Aβ plaque burden for age groups shown in **C**. Significance was calculated by a χ^2 statistic between the genotypes (**$P < 0.001$ and *$P < 0.01$). Error bars in **A** and **B** represents SEM for proportions for all PSAPP, but only select Tg2576 ($n = 4$) where a reasonable number of plaques were deposited. Error bars in **C** and **D** represent SD.

Quantitative Stereological Estimation of Dense Plaque-Vascular Association in Tg2576 and PSAPP Mice

Vascular relationship of the dense plaques was further explored by quantitative stereological techniques (Figure 3). Select plaques sampled systematically from neocortical and hippocampal regions of 14 Tg2576 and PSAPP mice (see above), and all plaques sampled from the entire brain hemisphere of Tg2576–24m and PSAPP-5m were analyzed on serial sections for plaque diameters, number of cores, and the number and caliber of associated vessels within an arbitrary distance of 4 μm between the plaque periphery and the adventitia of the vessel.

A statistically significant difference of means was observed between maximal diameters of dense plaques in Tg2576 (n = 466 plaques; mean diameter, 34.1 μm; range, 5.0 to 195.1 μm; SD, 23.23 μm) and PSAPP mice (n = 643 plaques; mean diameter, 25.6 μm; range, 5.1 to 89.7 μm; SD, 15.38 μm) ($P < 0.001$, CI = 6.2 to 10.8).

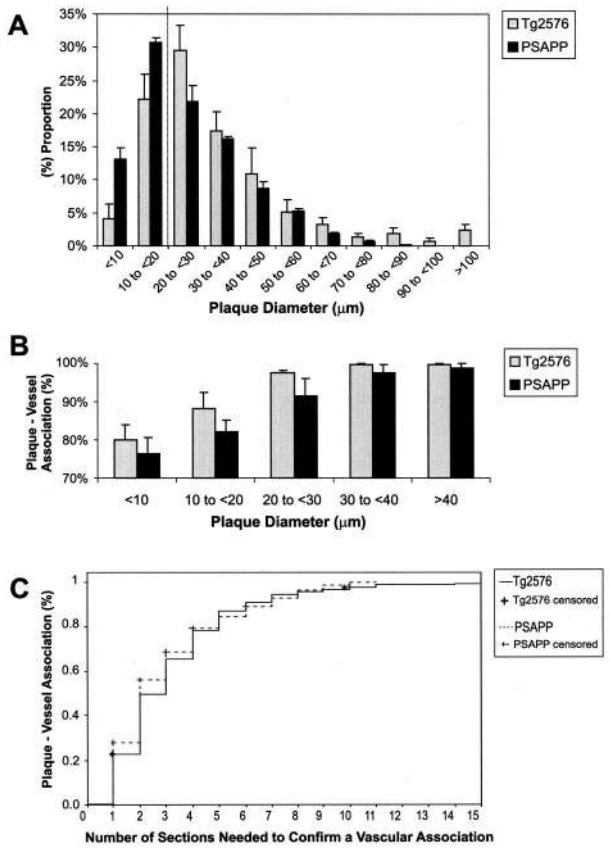

Figure 3. Morphometry in Tg2576 and PSAPP mice. **A:** Size distribution of dense plaques. **B:** Vascular association of dense plaques according to their sizes. **C:** Kaplan-Meier analysis suggested that in four to five sections (16 to 20 μm), >80% of plaques would appear to be associated with vessels at least once.

Size distribution of dense plaques showed that the modal diameter of plaques in PSAPP was smaller than 20 μm, whereas the majority of the plaques in Tg2576 were larger (Figure 3A). This difference was also consistent between Aβ burden-matched Tg2576–24m and PSAPP-5m (data not shown). Thus, PSAPP mice tended to have more numerous and smaller plaques than Tg2576 mice.

Analysis of the relationship between vessels and plaque sizes revealed >75% association for plaque diameters <10 μm in both Tg2576 and PSAPP mice. This association became stronger with increasing plaque diameter (Figure 3B). A strong correlation was observed between plaque diameter and number of associated vessels (Pearson's coefficient correlation, $r = 0.64$, $n = 1094$ plaques, $P < 0.001$). Twenty-one percent of plaques in Tg2576 were associated with vessels while significantly fewer plaques in PSAPP had vessels within them (5%; Pearson $\chi^2 = 64.5$, $P = <0.001$). The presence of vessels within plaques was dependent on plaque size. More than 50% of plaques larger than 60 μm had a vessel inside the plaque conglomerate or in one of its cores, and this number approached 100% in plaques larger than 100 μm for Tg2576 mice.

No correlation was observed between the caliber of the largest associated vessel and maximum plaque diameter or the diameter of individual plaque cores ($n = 1025$ plaques, Pearson's coefficient correlation, $r < 0.25$, $P < 0.001$). A strong correlation, however, was noted between the total number of cores and the total number of associated vessels (Pearson's coefficient correlation, $r = 0.65$, $P < 0.001$). A multivariate regression analysis showed that the association between the number of cores and vessels was independent of plaque size. Of all variables analyzed, the total number of associated vessels was the strongest predictor of the number of cores within a plaque (analysis of variance, regression SS = 2036, df = 2; residual SS = 1516, df = 1085; $F = 728.5$, $P < 0.001$). Furthermore, plaques showed an association with vessels within an average thickness of 11.8 μm (SD, 8.92 μm). This parameter did not differ between Tg2576 and PSAPP mice (Kaplan-Meier survival curve; log rank test, $P < 0.05$). Kaplan-Meier analysis further showed that in any given 4-μm section, 30% of the plaques were related to a vessel. If followed serially, ≈50% were positive in the next three to four sections. Some remained negative (Figure 3C).

Increased Association of Plaques with Vessels Is Not Incidental

A clear origin of dense plaques from vessel walls was noted for most plaques; however, ≈19 to 24% of the dense plaques (PSAPP/Tg2576) seem to originate from immediate perivascular regions. To confirm that this was not due to a chance association of plaques with the normal capillary network, the following experiments were performed. First, the mean vascular number and areas were measured for seven brain regions from 11- to 13-month-old nontransgenic, Tg2576, and PSAPP mice ($n = 2$, each) (Figure 4). To do this, sections were stained with GSL I-B_4, collagen IV, and an anti-mouse Ig. A strong correlation was observed between them (Pearson's coefficient correlation, $r \geq 0.84$, $P < 0.001$). For a total of 10,316 Ig-labeled vessels studied further, the mean vascular densities for nontransgenic, Tg2576, and PSAPP mice, were 529/mm^2 (SD, 87.2), 331/mm^2 (SD, 78.1), 467/mm^2 (SD, 85.3). A significantly decreased total vascular number and area was observed for Tg2576 compared to both PSAPP and nontransgenic mice (for all comparisons: $t > 4.6$, df = 82, $P < 0.001$). When studied in relation to brain regions, this difference was especially evident in the rhinal and frontal cortices (Pearson's χ^2 test, P at least <0.01). Based on these data, the average area covered by a single vessel and thus the maximum size of a single plaque that could occur within a distance of 4 μm with a probability of <0.05 was calculated. Our analysis showed that all plaques with a <20 μm diameter could not be explained by chance association, and for Tg2576 this could be as large as 80 μm.

In a second method, the vasculature was studied more closely with a variety of histochemical techniques in transgenic and control mice (Figure 5). On these sections, simulations were performed by randomly pitching circles of diameters 10, 20, and 40 μm to mimic plaques of various sizes. The circles had additional rims with radii exceeding

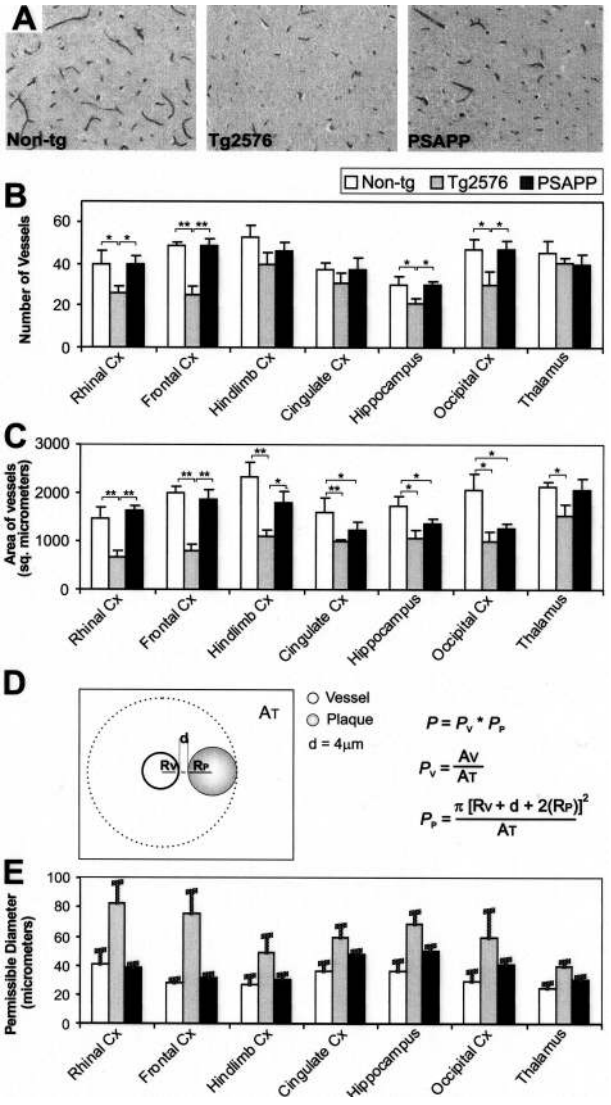

Figure 4. Vascular densities in nontransgenic, Tg2576, and PSAPP mice. **A:** Vessels stained by an anti-Ig for thalamus in 11- to 13-month-old nontransgenic, Tg2576, and PSAPP mice. **B** and **C:** Vessel densities were further calculated as number/area, and as area/area by densitometry. **D** and **E:** Based on both densities, the relative probability of encountering a vessel by chance was calculated as shown and bars represent the maximum size of the plaques at which they could occur in these regions without being associated with a vessel by chance. Error bars were calculated with SD of the mean vascular area (A_T).

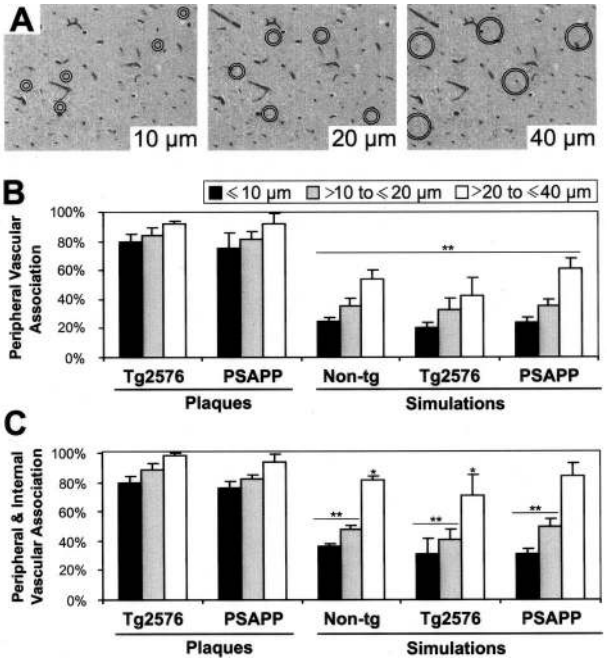

Figure 5. Simulation studies in nontransgenic, Tg2576, and PSAPP mice. **A:** An example of simulations of 10-μm, 20-μm, and of 40-μm ring composites assessing the relative chance of encountering vessels. **B** and **C:** Simulation for peripheral association with vessels (between the two **circles**) (**B**), or simulation for the situation when vessels are pushed outside the plaques (**C**, all vessels within the **outer circle**). Significance is calculated by Pearson's χ^2 test (**$P > 0.001$ and *$P < 0.01$). Error bars in **B** and **C** represent SEM. Notably, only those plaques that had a vascular association in all of the sections or none at all were included for this analysis because the control sections cannot be analyzed serially.

the first circle by 4 μm and vessels were counted within the rim area to mimic the arbitrary distance chosen for the positive association of plaques. A statistically significant difference was present between these simulations and the corresponding plaque sizes categorized in three groups (5 to <10 μm, 10 to <20 μm, and 30 to <40 μm) for both Tg2576 and PSAPP mice (Pearson's χ^2 test, $P < 0.001$). Next, plaques of the categorized sizes were compared with all vessels encompassed by the outer circle (rim area plus the area within the inner circle) to mimic the pushing model of amyloidogenesis in which developing plaques push the neuropil outside.[13] A similar analysis again showed a highly significant difference between the plaques and simulations for sizes 10 and 20 μm and a borderline significance for 40 μm (Pearson's χ^2 test, P at least <0.05). When the true sizes of plaques were taken into account, the differences were also significant for 40-μm diameter (analysis of variance, $P < 0.001$). Moreover, no statistical difference was observed between the vascular densities in APP, PSAPP, and nontransgenic mice with this methodology. Thus, the observed vascular association in Tg2576 and PSAPP mice cannot be attributed to chance.

Vessels Associate with All Dense Plaques in PSAPP Mice on Serial Semithin and Ultrathin Section Analysis

To address the significantly higher number of dense plaques in PSAPP mice not having a vascular relationship, we used 1-μm-semithin sections sliced from resin-embedded brains of 5- and 11-month-old PSAPP mice (Figure 6). Approximately 150 serial sections from each series were stained with methylene blue that only recognizes dense plaques as confirmed with Aβ immunohistochemistry. Furthermore, a morphometric analysis was performed for 100 plaques. Diameters of the plaques were assessed along with the sizes and number of individual central cores and the number of vessels. The mean diameter of senile plaques and of dense amyloid core was 54.7 μm (range, 14.7 to 103.8 μm; SD, 23.32) and 34.1 μm (range, 2.7 to 76.7 μm; SD, 21.58), respectively.

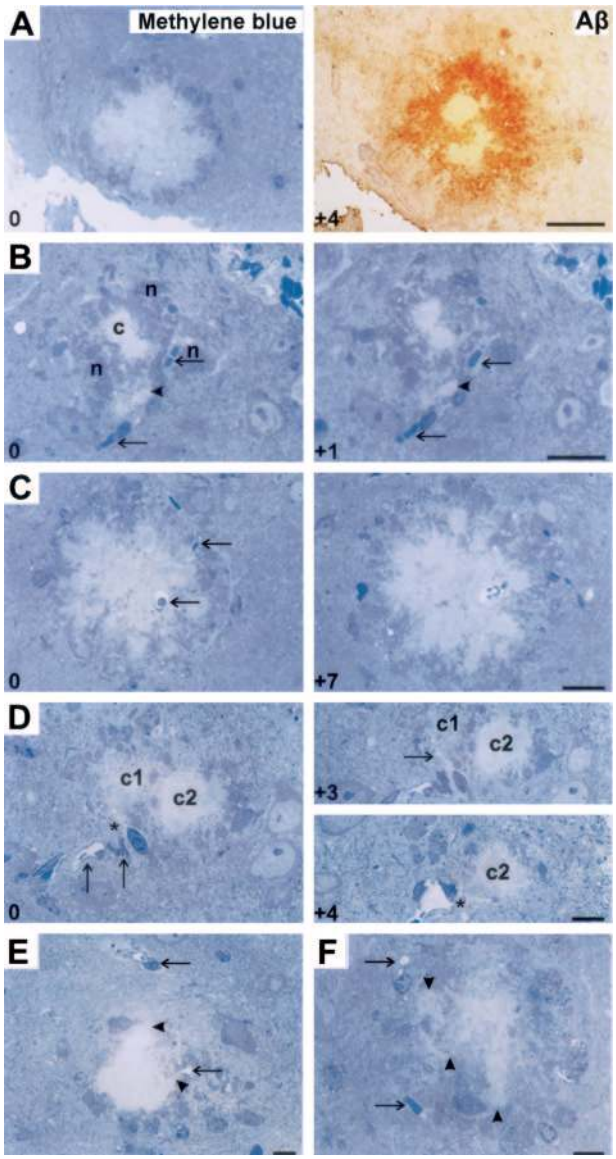

Figure 6. Semithin (1 μm thick) serial section analysis for PSAPP mice. Integers on the **bottom left corner** represent the relative sectional distance. **A:** Amyloid plaques on methylene blue staining were confirmed as dense-core plaques on histochemistry. **B:** Small dense deposit (**arrowhead**) developing in association with vessel wall (**arrows**) in close proximity to a senile plaque (c) surrounded by its neuritic elements (n). **C:** A dense plaque completely enclosing a vessel (**arrow**). **B** and **C** represent the first, mural-type of vascular association. **D:** Association of plaque c1 with perivascular space (*), the second type of vascular association. This converts to a mural-type of association in the following section (**arrow** in section marked +3). Similarly, plaque c2 with no relationship in section 0 developing a perivascular space association (*) in the section marked +4. **E** and **F** represent a third kind of vascular relationship in which growing edges of the plaques (**arrowheads**) extend toward vessels (**arrows**). Scale bars, 20 μm.

No plaque was identified that did not associate with a vessel at some level. For many dense amyloid cores, degenerated structures (vascular or neuritic) were also noted. The number of vessels had a strong correlation with the number of dense-core plaques (Pearson $\chi^2 = 72.4$, $P < 0.001$). This is despite the fact that the number of vessels was underrepresented because the same vessel was associated with a number of dense plaques on serial sections. In addition, we again noticed at least two types of plaque-vascular relationships. In the first (mural) type of association, circumscribed amyloid plaques studded the outer basal lamina of vessels. A single vessel could be shown to have many dense Aβ deposits in serial sections. Second, amyloid deposits originated from immediate perivascular parenchyma. Vessels at the periphery of plaques had focal vascular amyloid deposits, apparently adding new amyloid cores. In addition, a third type of vascular association was characterized by amyloid at the center of a plaque sending fine extensions toward a nonamyloidotic vessel. Directional amyloid growth was more consistently noted when a vessel was near, than when no vessels were observed.

Lastly, we attempted to identify the earliest Aβ deposits discernible by electron microscopy on serial sections sliced on formvar-coated single slot grids (Figure 7). All small fibrillar plaques observed originated from vessel walls. Aβ fibrils frequently stretched under the basement membrane toward the media-adventitial junction or into the perivascular space as observed earlier in AD.[35] Some fibrillar Aβ was evidenced in the neuropil but these were quite dispersed.

Loss of Endothelium and BBB Dysfunction in Tg2576 and PSAPP Mice

Based on a consistently decreased reactivity of a series of endothelial markers for Tg2576 and PSAPP mice brain vasculature, especially in the vicinity of Aβ deposits, we examined 5- and 11-month-old PSAPP female mice ultrastructurally (Figure 8). Both mice demonstrated all or some of these features: loss or thinning of endothelium, endothelial nuclear elongation, basement membrane thickening or splitting to accommodate Aβ, degeneration of smooth muscle cells, swelling of astroglial endfeet, degeneration of pericytes (or sometimes activation, with enlarged mitochondria), or a complete degeneration of microvessels. These features were not only evident in vessels that deposited Aβ in their walls but also in vessels that were free of Aβ deposits confirmed on immunogold labeling. Many of these vessels were either in close proximity to dense plaques in the same or serial sections, or observed to be curved or branching. Control nontransgenic mice up to 20 months of age did not show similar changes in the endothelium or other vascular structures (data not shown).

Earlier, age-related hemorrhagic stroke and microhemorrhages have been reported in APP23 mice.[36] We investigated whether Tg2576 and PSAPP mice also similarly encounter macro- or microhemorrhages. Of three mice that we lost during this study, one died just before being euthanized. Autopsy revealed a large cingulate-cortical bleed. Using the scoring system outlined in Materials and Methods, we further analyzed the combined prevalence of fresh and late microhemorrhages (by a H&E and a Prussian blue staining), scored by two investigators for 16 Tg2576 and PSAPP

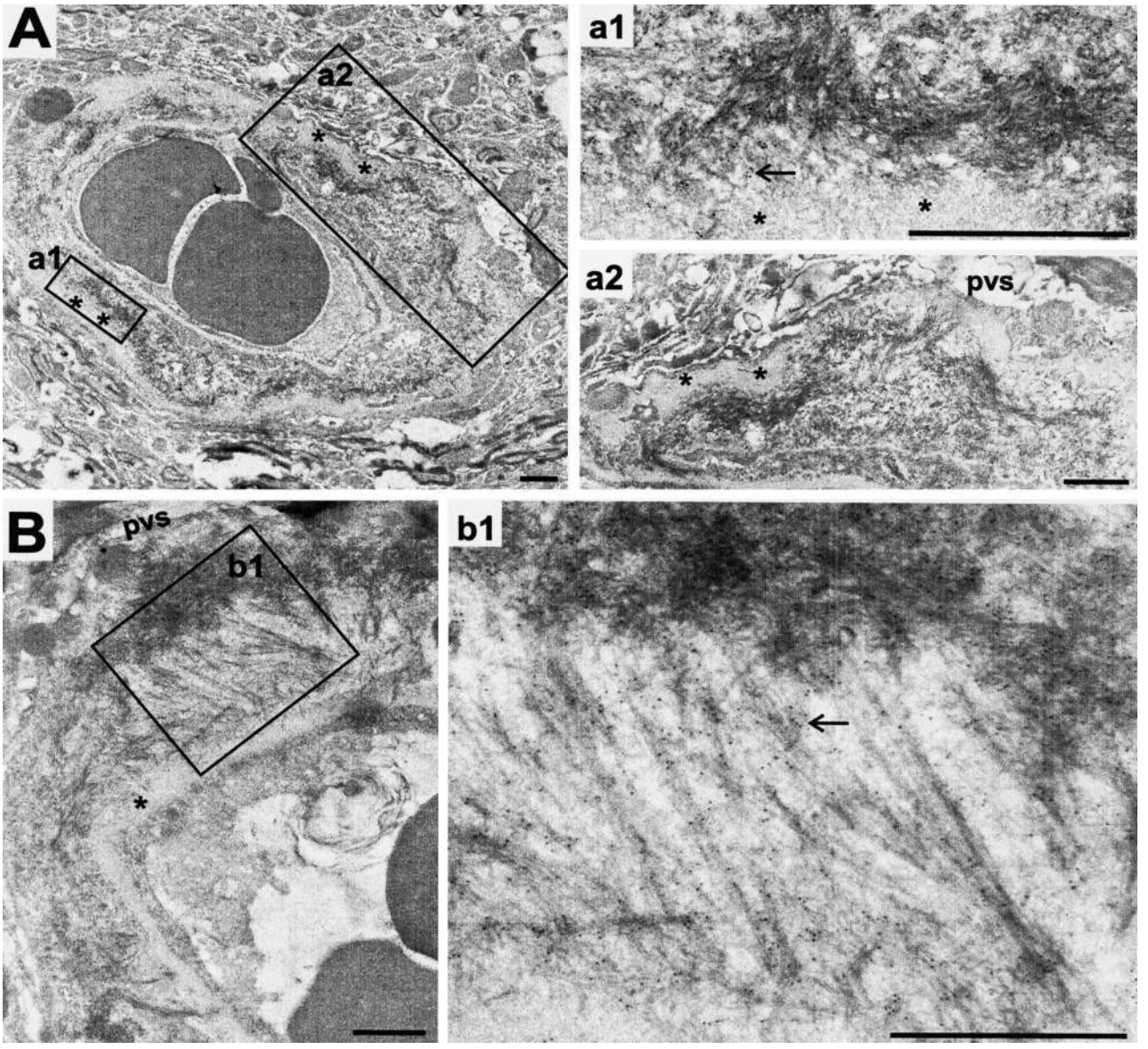

Figure 7. The earliest discernable Aβ aggregates recognized ultrastructurally by 10-nm gold particles on paraformaldehyde-fixed tissue. **A:** A 5-month-old PSAPP mouse depositing Aβ in a microvessel that seems to originate from the outer (abluminal) surface of the basement membrane and is contained within the thickened basal lamina (*). **B:** Similar vascular amyloid deposition in an 11-month-old PSAPP originating at the basement membrane and stretching toward the adventitia where it makes a focal dense deposit. Note the strong immunogold label for Aβ, **arrows**; pvs, perivascular space. Scale bars, 1 μm.

mice. A high concordance rate was observed between the investigators (Pearson's coefficient correlation, $r = 0.94$, $P < 0.001$) and the scores were further averaged. Transgenic mice grouped into young, adult, and old age groups, compared to age-matched controls showed a small, but a significantly higher score (mean score ± SEM in transgenic versus control: 0.20 ± 0.05 versus 0.05 ± 0.04 for young, 0.88 ± 0.11 versus 0.30 ± 0.11 for adult, and 0.43 ± 0.13 versus 0.50 ± 0.12 for the old age group; Pearson's χ^2 test, P at least <0.05). Importantly, microhemorrhages were not only present around CAA, but also around dense plaques.

We further questioned whether microvascular degeneration might have a more subtle functional consequence on BBB integrity. To assess this, we studied parenchymal infiltration of Ig and albumin serum proteins that are normally restricted by BBB. Sections were systematically sampled and scored as described above. A significantly higher scoring for all age groups versus age-matched controls was observed for albumin (0.60 ± 0.07 versus 0.10 ± 0.08 for young; 1.13 ± 0.12 versus 0.35 ± 0.12 for adult; 1.67 ± 0.14 versus 0.80 ± 0.16 for the old age group; Pearson's χ^2 test, $P < 0.05$) and for Ig immunolabeling (0.05 ± 0.04 versus 0.54 ± 0.06 for young; 0.30 ± 0.11 versus 1.05 ± 0.13 for adult; 0.50 ± 0.12 versus 1.73 ± 0.13 for the old age group; Pearson's χ^2 test, $P < 0.05$). Focal staining for Ig and albumin was frequently observed in what appeared as plaques although occasionally, neuronal surfaces were also stained.

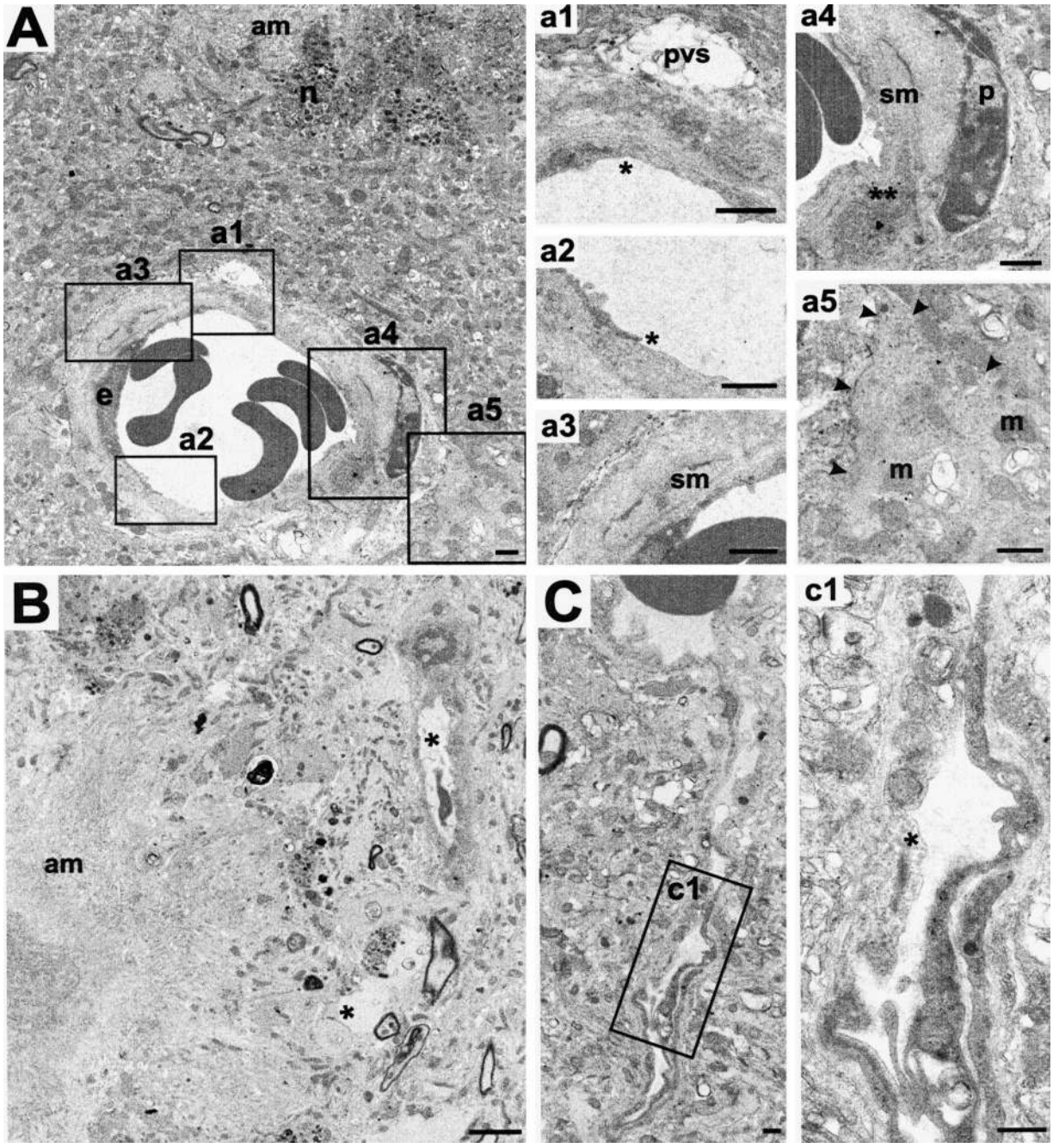

Figure 8. Vascular degenerative changes in PSAPP mice. **A:** Five-month-old PSAPP with a small arteriole in proximity to a dense amyloid plaque (am) showing endothelial loss (* in **a1** and **a2**), smooth muscle cell (sm) degeneration (** in **a4** and compare with the normal profile in **a3**), and slightly apparently swollen astroglial endfeet (edges marked by **arrowheads** in **a5**) (m, mitochondria; n, neuritic elements; pvs, perivascular space; p, pericytes). **B:** An 11-month-old PSAPP with degenerating vessels or vascular profiles (*) in the vicinity of an amyloid plaque (am). **C:** A 5-month-old PSAPP with an abnormal branching vessel distant from amyloid plaques demonstrating endothelial loss (*). Scale bars, 1 μm.

We further investigated the proportion of ThS or anti-Aβ labeled plaques for Ig and albumin staining for 16 Tg2576 and PSAPP mice (Figure 9). Ig or albumin labeling of dense plaques with either ThS or anti-Aβ showed good correlations (Pearson's coefficient correlations, $r \geq 0.91$, $P < 0.001$). For anti-Aβ-labeled plaques, an overall average of 2.4 to 18.2% showed Ig labeling and 1.8 to 16.6%, albumin staining. The proportion of dense plaques stained for serum proteins in the vicinity of microhemorrhages was close to 100% (Figure 9). On a multivariate linear regression analysis the presence of microhemorrhages or of serum proteins in Tg2576, PSAPP, and nontransgenic mice independently increased with age and ThS burden (analysis of variance, age: $F \geq 11$, $P < 0.001$; ThS: $F \geq 9$, $P < 0.01$). Because age emerged as one of the predictors,

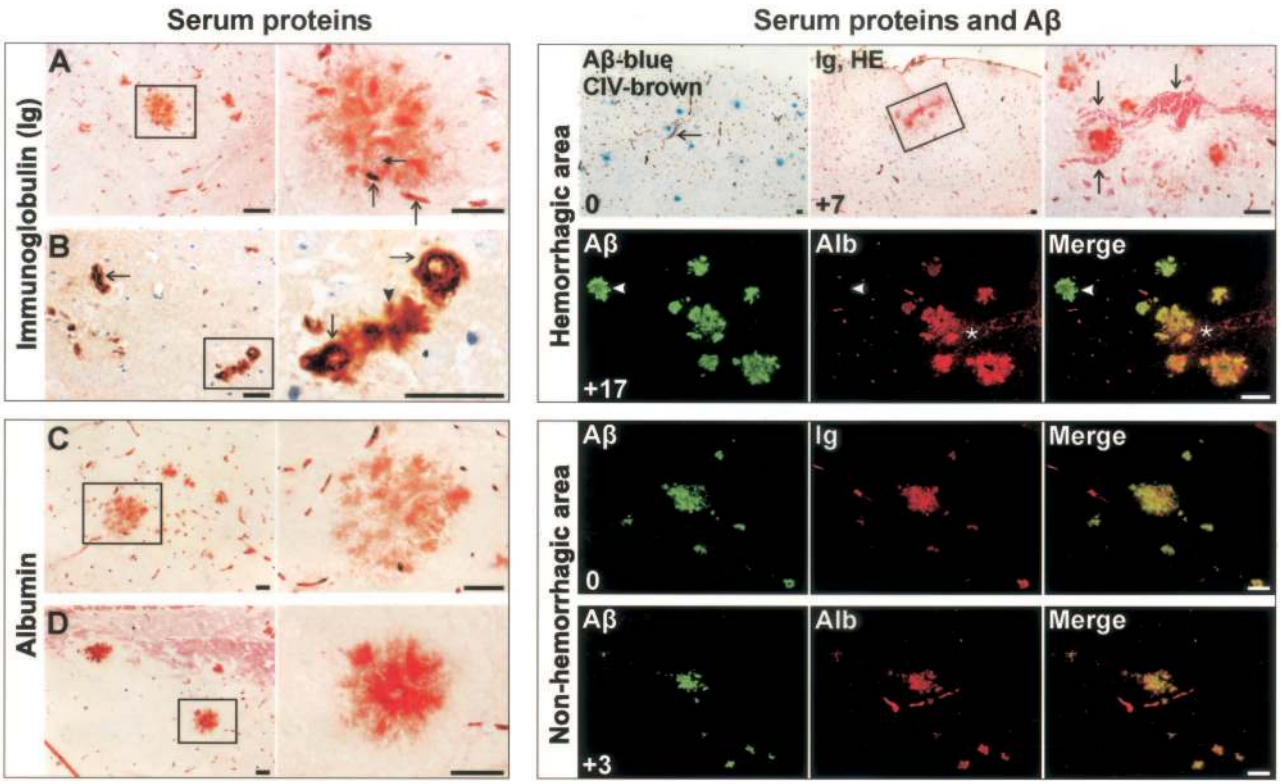

Figure 9. Staining for serum proteins for dense plaques. **Left**: **A:** A 24-month-old Tg2576 showing Ig staining of dense plaques in hippocampal region associated with vessels (**arrows**). A **doubleheaded arrow** points to a vessel within plaque. **B:** Amyloid angiopathy in thalamus of the same mouse again showing Ig staining of the abluminal surface of CAA (**arrows**) as well as of the associated plaque (**arrowhead**). **C** and **D:** Albumin staining in various brain regions of the same mouse. **Right**: Integers on the **bottom left corner** represent the relative sectional distance. Serum proteins co-localized with Aβ plaques in a hemorrhagic area (**arrows** and **asterisks**) of a 17-month-old Tg2576 studied by light and fluorescent microscopy. **Arrowhead** points to a plaque distant from hemorrhage not infiltrated by serum proteins. However, infiltration of dense plaques by serum proteins in nonhemorrhagic areas also occurred as shown here in a cortical region of an elderly 25-month-old Tg2576. Scale bars, 40 μm.

no intercomparisons were made between Tg2576 and PSAPP mice that were well balanced for Aβ burden, but not for age.

Discussion

Dense Amyloid Deposits in AD Mice Are Derived from Vessel Walls

A precise understanding of the development of different forms of plaques, especially those that are thought to contribute to AD pathology, is crucial for devising therapeutic approaches to retard or reverse this devastating disease. Here we show that dense Aβ deposits are developmentally related to vessels in two well studied and partly independent models of amyloidosis. Systematically analyzed different brain regions from a panel of Tg2576 and PSAPP mice of different age groups first showed that ≈85 to 94% of dense plaques in PSAPP/Tg2576 mice are associated with vessels, a relationship that was consistent for different brain regions, genetic backgrounds, gender, and to some extent, age and amyloid burden. Because the appearance and prevalence of dense Aβ deposits, including CAA, might vary in different brain regions of these and other AD models,[31,36] we further analyzed the entire brain region of one each of Tg2576 and PSAPP mice. Again, ≈85 to 96% of dense plaques in PSAPP/Tg2576 mice were associated with vessels. Modeling and simulation studies suggested that for plaques up to 40 μm in diameter (constituting >70% plaques in Tg2576 and >80% in PSAPP mice), the observed vascular associations were not due to chance. To further strengthen our data, we studied dense plaques ≤20 μm diameter from one of the youngest Tg2576 that barely deposit Aβ. Using collagen IV alone, a vascular marker that does not consistently recognize all small capillaries, ≈81% of the dense plaques were positively associated with vessels.

This is the first report addressing a vascular relationship of Aβ plaques in mouse models of AD. Earlier studies in humans have suggested or demonstrated a vascular origin of senile plaques or diffuse plaques.[7–12,14,15,35] Our study differs from these on three counts: 1) we addressed plaques occurring in AD mouse models; 2) we studied only dense Aβ deposits and excluded diffuse plaques from our analyses; and, 3) we did not exclude association with capillaries >10 μm as Kawai and colleagues[13] did. Indeed, we showed a frequent occurrence of dyshoric angiopathy involving terminal arterioles (defined as vessels with lumen diameter <50 μm) and occasionally, even larger muscular arterioles.

Although we show that most dense Aβ deposits are associated with vessels in mouse models of AD, we also suggest a vascular-related temporal sequence in their evolution. For instance, it might be argued that diffuse plaques develop first and those that are traversed by vessels evolve into dense plaques. However, if this indeed occurs, it is a rapid phenomenon as even in the youngest Tg2576 mice analyzed here that barely deposited Aβ, the majority of the dense plaques were already formed. These data are consistent with similar observations made on young PSAPP mice,[23,24,31] suggesting that the majority of the ThS-positive plaques might not pass through a detectable diffuse stage on their way to becoming dense plaques.[31] We also confirmed this in older mice that deposited robust Aβ. Serial 1-μm-thin section analysis of 5- and 11-month-old PSAPP mice with dyes that do not recognize diffuse Aβ, showed that all dense deposits occurred in association with vessel walls or in the immediate perivascular regions. A further search by electron microscopy for the earliest compact fibrillar structures, with the aid of Aβ immunogold labeling, pointed again toward vessel walls being the nidi for most dense plaques. And lastly, the notion that dense-core plaques are developmentally distinct from diffuse plaques in Tg2576 and PSAPP is also supported by observations that the majority of small dense plaques lacked surrounding diffuse amyloid, which otherwise would have been expected if part of a diffuse plaque underwent compaction to form a dense plaque.

In a 20-month-old PSAPP mouse, only $\approx$75% of the dense plaques were associated with vessels. It has been previously shown that the proportion of ThS-positive plaques in aging PSAPP mice increase while immunohistochemically detected Aβ remains constant.[32] We did not analyze PSAPP mice $>$11 months by semithin or ultrastructural microscopy, therefore a possibility exists that some diffuse plaques in these elderly PSAPP mice might have been converted to ThS-positive plaques.

Tg2576 and PSAPP Mice Have BBB Dysfunction as Described in AD

By 5 months of age, PSAPP mice have a number of ultrastructural vascular abnormalities, including endothelial loss, basement membrane thickening, loss of smooth muscle cells, and pericytic degeneration. Some vessels were completely degenerated. Besides amyloidotic vessels, these changes were also pronounced in vessels that were in the direct vicinity of plaques; however, loss of endothelial cells was also observed in vessels free of amyloid and distant from plaques, some of which were curved or branched. The curved or branching vascular segments are proposed to be prone to shear stress due to an alteration in blood flow,[37] although toxicity of soluble Aβ on endothelial cells[38] could also contribute significantly to the endothelial degenerative changes observed here. Interestingly, these aspects have a close resemblance to AD pathology in which a wide variety of structural microvascular abnormalities have been observed to correlate with the number of senile plaques, including loss of endothelial cell markers CD31 and CD34,[39] basement membrane thickening,[40] and astrogliosis, among others.[4,26]

We further showed that these ultrastructural microvascular abnormalities are associated with functional impairments of the BBB especially in the vicinity of microvessel-related dense Aβ deposits. Although occurrence of hemorrhages in Tg2576 and PSAPP mice was significantly more than age-matched nontransgenic mice, such phenomena were not observed to be very frequent. On the other hand, using immunohistochemical approaches, we observed a recurrent extravasation of serum proteins, normally restricted by BBB, in the neuropil. Presence of Ig or albumin was observed in up to 18% of dense Aβ deposits for any mouse examined. These observations were more consistent in older mice and especially in those regions that also had hemorrhages. By contrast, a minimal or no BBB leakage was observed in nontransgenic mice.[41] Moreover, we suspect that these plasma extravasations are rather subtle and transient, escaping detection by isotopic permeability studies.[42]

Vasocentric Dense Plaques in Tg2576 and PSAPP Resemble Flemish AD Pathology

Despite having abundant CAA, sporadic AD patients do not commonly have strokes. The described pathology for Tg2576 and PSAPP best resemble Flemish AD pathology characterized by vascular hemorrhage and dementia. These patients present with the largest dense-core plaques reported in AD that are also multicentric as described here for Tg2576 and PSAPP mice.[15,19,43] Moreover, we recently showed that a majority of dense-core plaques in Flemish AD patients are directly associated with vessel walls.[15] The observed resemblance of plaque origin and morphology between the Flemish AD and Tg2576/PSAPP mice also has a biochemical basis. Earlier studies have suggested that despite the fact that PSAPP mice have elevated levels of Aβ42 on both enzyme-linked immunosorbent assay[44] and on mass spectrometry[31] than Tg2576, both PSAPP and Tg2576 have at least twofold higher Aβ40 levels than Aβ42.[31] This although is in sharp contrast to AD and Down's syndrome patients,[4,45] interestingly, a mass spectrometric analysis of Flemish AD brain has also revealed a preponderance of Aβ40.[15] Table 1 summarizes these similarities. It is also not yet clear to which extent the plaque-vascular relationship exists for human nonvariant AD. For one, the transgenic mice studied here secrete supraphysiological amounts of Aβ and because vessels are a normal path of clearance (see next section), mice might be skewed to have dense plaque formation around vessels. Furthermore, some unique components of murine vasculature might also interact with human Aβ, either enriching it in this compartment, or directly creating or maintaining the seed. Specific gangliosides could be one factor that has been shown to seed plaque deposition.[46]

Table 1. Morphological and Biochemical Comparison of Aβ Plaques Observed in Tg2576 and PSAPP Mouse Models of AD, and Human Nonvariant AD as Well as Flemish AD

	Tg2576 (old)	PSAPP	Flemish AD patients	AD and Down's syndrome patients
Dense plaque characteristics:				
Large dense cores	++++	+++	+++	+
Multicentric dense cores	++++	++++	+++	+
Neuritic	+	+	+++	+++
Vasocentric	++++	+++	+++	±
CAA	++ to +++	++ to +++	+++	+ to +++
Dyshoric angiopathy involving larger arterioles	++ to +++	+ to ++	++ to +++	+
Diffuse plaques	+	++	++	+++
Aβ C-terminus	Aβ40>>Aβ42 (31)	Aβ40>Aβ42 (31)	Aβ40>>Aβ42 (15)	Aβ40<Aβ42

Microvessels Play a Central Role in the Observed Pathology of Mouse Models of AD

Recent work on transgenic mice has provided evidence that Aβ existing in monomeric or soluble form in the parenchymal interstitial fluid undergoes varied fates involving macrophage uptake and degradation by cellular or extracellular proteases.[47–49] Some Aβ (predominantly Aβ42) is readily deposited at the sites of production as diffuse plaques and the remaining Aβ diffuses passively following Fick's diffusion principle, suggested by the presence of Aβ at sites distant from its production.[50,51] Evidence also suggests that diffusing, soluble Aβ may be cleared out of brain by two pathways associated with blood vessels. One of these mechanisms is a direct Aβ transport across the BBB mediated by LDL receptor-related protein-1 (LRP-1), which in turn is influenced by α2-macroglobulin and ApoE.[52] This is a highly efficient mechanism of brain Aβ clearance not only in young animals, but also in partly clearing pathological amounts of Aβ in mouse AD models.[53] Another vessel-related Aβ clearance is along the periarterial interstitial fluid drainage pathways from where Aβ reaches cerebrospinal fluid and is eventually drained into the systemic circulation. Tracer experiments demonstrate that this is equivalent to lymphatics of brain,[54] and might be a major route of Aβ elimination in older animals when the Aβ transport across BBB becomes less efficient[52] or when this pathway is overwhelmed as in mouse AD models.[51,54] And lastly, Aβ transport across the BBB is bidirectional with Aβ from blood also being actively transported across the BBB with the receptor for advanced glycation end products (RAGE).[55]

The present evidence that dense plaques in Tg2576 and PSAPP mice are centered on vessel walls suggests that Aβ may be deposited during clearance by vascular or perivascular drainage pathways. Formation of CAA in these mouse AD models has been earlier proposed to be due to Aβ entrapment in the periarterial interstitial fluid drainage path.[51,54,56] How this precisely happens is currently unknown. The observations that PSAPP mice have more numerous but significantly smaller dense plaques than Tg2576 mice support the premise that Aβ42 is important in seeding dense plaques. This nidus could either be provided directly by vascular components[57] or by diffusing Aβ interaction with specific vascular chaperones that facilitate its growth along or within vessel walls and result in classical CAA. However, in the presence of other local factors (ie, bulk Aβ flow; see below), the initial vascular nidus might further sequester diffusing Aβ and grow back into the parenchyma as dyshoric angiopathy or dense plaques.

The evidence that predominantly neuronally derived Aβ in Tg2576 and PSAPP mice deposits in association with vessels as CAA[51,54,56] or dense plaques (this study) suggests that soluble Aβ migrates toward vessels (Figure 10). If the clearance across the BBB is highly efficient as suggested,[53] this could be an important factor in maintaining an Aβ gradient between neurons and vessels. Moreover, this gradient may be specific for Aβ40 as LRP-mediated BBB transport clears Aβ40 more efficiently than Aβ42.[58] Interestingly, Aβ40 is also the major constituent of both types of dense deposits (dense plaques and CAA) in Tg2576 and PSAPP mice.[23,31] Furthermore, a slight, but significantly higher proportion of vascular association noted for dense Aβ plaques occurring in Tg2576 mice, also showing a higher Aβ40 burden,[31] suggest that Aβ40 plays a pivotal role in dense-plaque formation. Interestingly, amyloid polymerization has been shown to occur by monomer addition in a reaction distinct from, and competitive with, formation of oligomeric intermediates.[59] Perhaps, the low fibrillogenic potential of Aβ40 along with its specific vascular clearance mechanisms facilitates its migration toward vessels where it is polymerized on the existing plaques by monomer addition. Additional support for an evolutionarily conserved pathway for clearance of Aβ40 by vessels is the observation that neprilysin does not degrade Aβ40 *in vivo* as efficiently it does Aβ42.[60]

Additionally, RAGE can transport Aβ from the blood to the abluminal endothelial surface[55] and further the growth of plaques especially when the normal brain to vessel clearance gradient is lost as can occur during aging.[52] Another factor that could lead to disruption of Aβ clearance is down-regulation of LRP expression or Aβ-mediated proteasome degradation of LRP in vascular endothelium.[55] We propose that a compromised BBB may contribute to Aβ clearance as well as to the growth of vessel-associated plaques when the LRP-mediated Aβ efflux is lost or hindered. In the absence of an intact BBB,

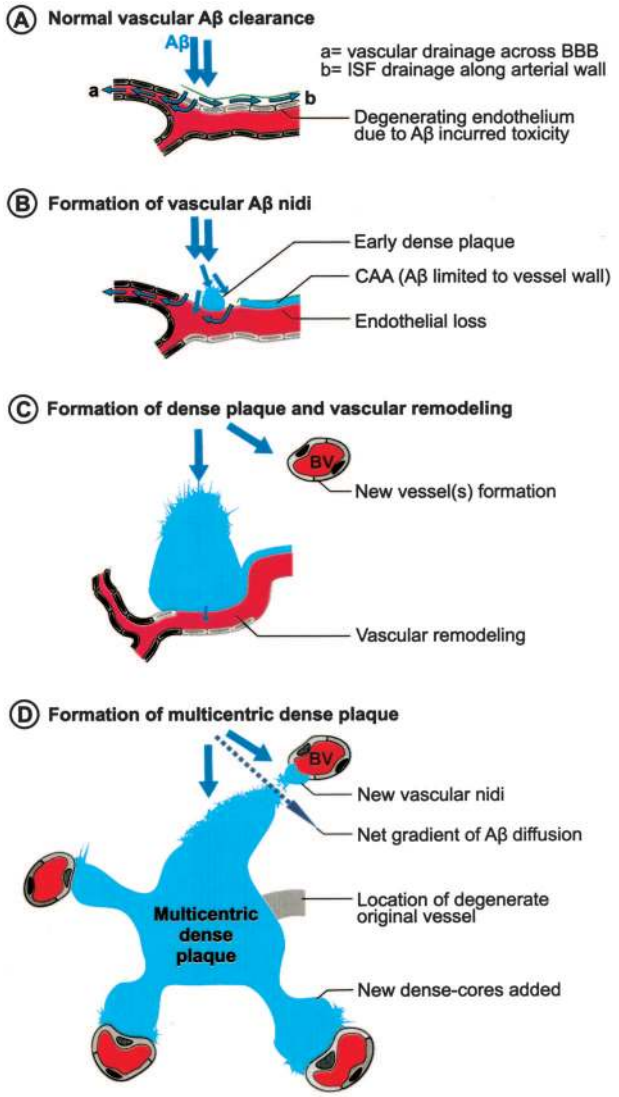

Figure 10. Model for dense plaque formation in Tg2576 and PSAPP mice. **A:** The majority of secreted Aβ not degraded or deposited as diffuse plaques is cleared through the blood vessels that set the major gradient of Aβ flow. **B:** Perturbed vascular clearance, also facilitated by local perivascular enrichment, causes early Aβ nidus formation as has been earlier proposed in the formation of CAA. Importantly, although Aβ down-regulates its own active efflux (ie, by LRP loss), but concurrent damage to the endothelium maintains its passive vascular clearance and neuron to vessel gradient of Aβ diffusion. **C:** Vascular remodeling occurs to maintain cerebral perfusion and to accommodate the dense plaques that enlarge by further sequestering Aβ. **D:** However, the gradient of Aβ clearance shifts toward new vessels that form as a result of vascular remodeling and together with dense plaques set the axis in which the soluble Aβ diffuses (**striped arrow**). Eventual involvement of the new vessels result in multicentric dense-core plaques.

plasma Aβ can accelerate the growth of dense plaques. Conversely, Aβ may be cleared directly into the blood depending on the equilibrium between blood and brain Aβ. All this fits well with evidence that Aβ accumulates in brain as blood levels of Aβ fall, and this clearance is greatly increased by the peripheral sequestering of Aβ by immune[61] or nonimmune[55,62] mechanisms.

Notwithstanding the precise mechanism of formation, the present study, for the first time, demonstrates that dense amyloid plaques in Tg2576 and PSAPP mice are centered on vessel walls. If a similar mechanism is also operative in AD, therapeutics targeting Aβ clearance from the vascular compartment may be most beneficial.

Acknowledgments

We thank Dr. Karen Hsiao for the gift of Tg2576; and Mrs. L. De Wit, U. Lübke, and I. Bats for expert electron microscopy assistance.

References

1. Hardy JA, Higgins GA: Alzheimer's disease: the amyloid cascade hypothesis. Science 1992, 256:184–185
2. Van Broeckhoven C: Molecular genetics of Alzheimer disease: identification of genes and gene mutations. Eur Neurol 1995, 35:8–19
3. Selkoe DJ: The cell biology of β-amyloid precursor protein and presenilin in Alzheimer's disease. Trends Cell Biol 1998, 8:447–453
4. Dickson DW: The pathogenesis of senile plaques. J Neuropathol Exp Neurol 1997, 56:321–339
5. Yankner BA, Duffy LK, Kirschner DA: Neurotrophic and neurotoxic effects of amyloid beta-protein—reversal by tachykinin neuropeptides. Science 1990, 250:279–282
6. Joachim CL, Morris JH, Selkoe DJ: Clinically diagnosed Alzheimers-disease—autopsy results in 150 cases. Ann Neurol 1988, 24:50–56
7. Scholtz W: Studien zur Pathologie der Hirngefässe. II. Die drüsige Entartung der Hirnarterien und-capillären. Z Gesamte Neurol Psychiat 1938, 162:694–715
8. Ishii T: Enzyme histochemical studies of senile plaques and the plaque-like degeneration of arteries and capillaries (Scholz). Acta Neuropathol (Berl) 1969, 14:250–260
9. Mandybur TI: The incidence of cerebral amyloid angiopathy in Alzheimer's disease. Neurology 1975, 25:120–126
10. Glenner GG: Amyloid deposits and amyloidosis. N Engl J Med 1980, 302:1283–1292
11. Miyakawa T, Shimoji A, Kuramoto R, Higuchi Y: The relationship between senile plaques and cerebral blood vessels in Alzheimer's disease and senile dementia. Morphological mechanism of senile plaque production. Virchows Arch B Cell Pathol Incl Mol Pathol 1982, 40:121–129
12. Arai H, Sagi N, Noguchi I, Haga S, Ishii T, Makino Y, Kosaka K: An immunohistochemical study of beta-protein in Alzheimer-type dementia brains. J Neurol 1989, 236:214–217
13. Kawai M, Kalaria RN, Harik SI, Perry G: The relationship of amyloid plaques to cerebral capillaries in Alzheimer's disease. Am J Pathol 1990, 137:1435–1446
14. Iwamoto N, Nishiyama E, Ohwada J, Arai H: Distribution of amyloid deposits in the cerebral white matter of the Alzheimer's disease brain: relationship to blood vessels. Acta Neuropathol (Berl) 1997, 93:334–340
15. Kumar-Singh S, Cras P, Wang R, Kros JM, van Swieten J, Lubke U, Ceuterick C, Serneels S, Vennekens K, Timmermans J-P, Van Marck E, Martin J-J, van Duijn C, Van Broeckhoven C: Dense-core senile plaques in the Flemish variant of Alzheimer's disease are vasocentric. Am J Pathol 2002, 161:507–520
16. Vinters HV, Wang ZZ, Secor DL: Brain parenchymal and microvascular amyloid in Alzheimer's disease. Brain Pathol 1996, 6:179–195
17. Morel F, Wildi E: General and cellular pathochemistry of senile and presenile alterations of the brain. Proc 1st Int Cong Neuropathol Rome 1952, 347–374
18. Peers MC, Lenders MB, Defossez A, Delacourte A, Mazzuca M: Cortical angiopathy in Alzheimers-disease—the formation of dystrophic perivascular neurites is related to the exudation of amyloid fibrils from the pathological vessels. Virchows Arch A Pathol Anat Histopathol 1988, 414:15–20
19. Hendriks L, van Duijn CM, Cras P, Cruts M, Van Hul W, van Harskamp F, Warren A, McInnis MG, Antonarakis SE, Martin J-J, Hofman A, Van Broeckhoven C: Presenile dementia and cerebral haemorrhage linked to a mutation at condon 692 of the β-amyloid precursor protein gene. Nat Genet 1992, 1:218–221
20. Dermaut B, Kumar-Singh S, De Jonghe C, Cruts M, Lofgren A, Lubke

U, Cras P, Dom R, De Deyn PP, Martin JJ, Van Broeckhoven C: Cerebral amyloid angiopathy is a pathogenic lesion in Alzheimer's disease due to a novel presenilin 1 mutation. Brain 2001, 124:2383–2392
21. Games D, Adams D, Alessandrini R, Barbour R, Berthelette P, Blackwell C, Carr T, Clemens J, Donaldson T, Gillespie F, Guido T, Hagopian S, Johnsonwood K, Khan K, Lee M, Leibowitz P, Lieberburg I, Little S, Masliah E, McConlogue L, Montoyazavala M, Mucke L, Paganini L, Penniman E, Power M, Schenk D, Seubert P, Snyder B, Soriano F, Tan H, Vitale J, Wadsworth S, Wolozin B, Zhao J: Alzheimer-type neuropathology in transgenic mice overexpressing V717F beta-amyloid precursor protein. Nature 1995, 373:523–527
22. Hsiao K, Chapman P, Nilsen S, Eckman C, Harigaya Y, Younkin S, Yang F, Cole G: Correlative memory deficits, Abeta elevation, and amyloid plaques in transgenic mice. Science 1996, 274:99–102
23. Holcomb L, Gordon MN, McGowan E, Yu X, Benkovic S, Jantzen P, Wright K, Saad I, Mueller R, Morgan D, Sanders S, Zehr C, O'Campo K, Hardy J, Prada CM, Eckman C, Younkin S, Hsiao K, Duff K: Accelerated Alzheimer-type phenotype in transgenic mice carrying both mutant amyloid precursor protein and presenilin 1 transgenes. Nat Med 1998, 4:97–100
24. Sturchler-Pierrat C, Abramowski D, Duke M, Wiederhold KH, Mistl C, Rothacher S, Ledermann B, Burki K, Frey P, Paganetti PA, Waridel C, Calhoun ME, Jucker M, Probst A, Staufenbiel M, Sommer B: Two amyloid precursor protein transgenic mouse models with Alzheimer disease-like pathology. Proc Natl Acad Sci USA 1997, 94:13287–13292
25. Urbanc B, Cruz L, Le R, Sanders J, Ashe KH, Duff K, Stanley HE, Irizarry MC, Hyman BT: Neurotoxic effects of thioflavin S-positive amyloid deposits in transgenic mice and Alzheimer's disease. Proc Natl Acad Sci USA 2002, 99:13990–13995
26. Farkas E, Luiten PGM: Cerebral microvascular pathology in aging and Alzheimer's disease. Prog Neurobiol 2001, 64:575–611
27. Duff K, Eckman C, Zehr C, Yu X, Prada CM, Perez-tur J, Hutton M, Buee L, Harigaya Y, Yager D, Morgan D, Gordon MN, Holcomb L, Refolo L, Zenk B, Hardy J, Younkin S: Increased amyloid-beta42(43) in brains of mice expressing mutant presenilin 1. Nature 1996, 383:710–713
28. Kumar-Singh S, De Jonghe C, Cruts M, Kleinert R, Wang R, Mercken M, De Strooper B, Vanderstichele H, Lofgren A, Vanderhoeven I, Backhovens H, Vanmechelen E, Kroisel PM, Van Broeckhoven C: Nonfibrillar diffuse amyloid deposition due to a gamma(42)-secretase site mutation points to an essential role for N-truncated abeta(42) in Alzheimer's disease. Hum Mol Genet 2000, 9:2589–2598
29. Kumar-Singh S, Vermeulen PB, Weyler J, Segers K, Weyn B, Van Daele A, Van Oosterom AT, Dirix LY, Van Marck E: Evaluation of tumour angiogenesis as a prognostic marker in malignant mesothelioma. J Pathol 1997, 182:211–216
30. Maxwell MH: Two rapid and simple methods for the removal of resins from 1.0 micrometer thick epoxy sections. J Microsc 1977, 112:253–255
31. McGowan E, Sanders S, Iwatsubo T, Takeuchi A, Saido T, Zehr C, Yu X, Uljon S, Wang R, Mann D, Dickson D, Duff K: Amyloid phenotype characterization of transgenic mice overexpressing both mutant amyloid precursor protein and mutant presenilin 1 transgenes. Neurobiol Dis 1999, 6:231–244
32. Matsuoka Y, Picciano M, Malester B, LaFrancois J, Zehr C, Daeschner JM, Olschowka JA, Fonseca MI, O'Banion MK, Tenner AJ, Lemere CA, Duff K: Inflammatory responses to amyloidosis in a transgenic mouse model of Alzheimer's disease. Am J Pathol 2001, 158:1345–1354
33. Callahan MJ, Lipinski WJ, Bian F, Durham RA, Pack A, Walker LC: Augmented senile plaque load in aged female beta-amyloid precursor protein-transgenic mice. Am J Pathol 2001, 158:1173–1177
34. Wang J, Tanila H, Puolivali J, Kadish I, van Groen T: Gender differences in the amount and deposition of amyloid beta in APPswe and PS1 double transgenic mice. Neurobiol Disease 2003, 14:318–327
35. Yamaguchi H, Yamazaki T, Lemere CA, Frosch MP, Selkoe DJ: Beta amyloid is focally deposited within the outer basement membrane in the amyloid angiopathy of Alzheimer's disease. An immunoelectron microscopic study. Am J Pathol 1992, 141:249–259
36. Winkler DT, Bondolfi L, Herzig MC, Jann L, Calhoun ME, Wiederhold KH, Tolnay M, Staufenbiel M, Jucker M: Spontaneous hemorrhagic stroke in a mouse model of cerebral amyloid angiopathy. J Neurosci 2001, 21:1619–1627
37. de la Torre JC: Is Alzheimer's disease a neurodegenerative or a vascular disorder? Data, dogma, and dialectics. Lancet Neurol 2004, 3:184–190
38. Thomas T, Thomas G, McLendon C, Sutton T, Mullan M: Beta-amyloid-mediated vasoactivity and vascular endothelial damage. Nature 1996, 380:168–171
39. Kalaria RN, Hedera P: Differential degeneration of the cerebral microvasculature in Alzheimer's disease. Neuroreport 1995, 6:477–480
40. Perlmutter LS, Chui HC: Microangiopathy, the vascular basement-membrane and Alzheimers-disease—a review. Brain Res Bull 1990, 24: 677–686
41. Mooradian AD: Effect of aging on the blood-brain-barrier. Neurobiol Aging 1988, 9:31–39
42. Poduslo JF, Curran GL, Wengenack TM, Malester B, Duff K: Permeability of proteins at the blood-brain barrier in the normal adult mouse and double transgenic mouse model of Alzheimer's disease. Neurobiol Disease 2001, 8:555–567
43. Cras P, van Harskamp F, Hendriks L, Ceuterick C, van Duijn CM, Stefanko SZ, Hofman A, Kros JM, Van Broeckhoven C, Martin JJ: Presenile Alzheimer dementia characterized by amyloid angiopathy and large amyloid core type senile plaques in the APP 692Ala–>Gly mutation. Acta Neuropathol 1998, 96:253–260
44. Holcomb L, Gordon MN, McGowan E, Yu X, Benkovic S, Jantzen P, Wright K, Saad I, Mueller R, Morgan D, Sanders S, Zehr C, O'Campo K, Hardy J, Prada CM, Eckman C, Younkin S, Hsiao K, Duff K: Accelerated Alzheimer-type phenotype in transgenic mice carrying both mutant amyloid precursor protein and presenilin 1 transgenes. Nat Med 1998, 4:97–100
45. Lemere CA, Blusztajn JK, Yamaguchi H, Wisniewski T, Saido TC, Selkoe DJ: Sequence of deposition of heterogeneous amyloid beta-peptides and APO E in Down syndrome: implications for initial events in amyloid plaque formation. Neurobiol Dis 1996, 3:16–32
46. Hayashi H, Kimura N, Yamaguchi H, Hasegawa K, Yokoseki T, Shibata M, Yamamoto N, Michikawa M, Yoshikawa Y, Terao K, Matsuzaki K, Lemere CA, Selkoe DJ, Naiki H, Yanagisawa K: A seed for Alzheimer amyloid in the brain. J Neurosci 2004, 24:4894–4902
47. Savage MJ, Trusko SP, Howland DS, Pinsker LR, Mistretta S, Reaume AG, Greenberg BD, Siman R, Scott RW: Turnover of amyloid beta-protein in mouse brain and acute reduction of its level by phorbol ester. J Neurosci 1998, 18:1743–1752
48. Selkoe DJ: Clearing the brain's amyloid cobwebs. Neuron 2001, 32:177–180
49. Tucker HM, Kihiko M, Caldwell JN, Wright S, Kawarabayashi T, Price D, Walker D, Scheff S, McGillis JP, Rydel RE, Estus S: The plasmin system is induced by and degrades amyloid-beta aggregates. J Neurosci 2000, 20:3937–3946
50. Meyer-Luehmann M, Stalder M, Herzig MC, Kaeser SA, Kohler E, Pfeifer M, Boncristiano S, Mathews PM, Mercken M, Abramowski D, Staufenbiel M, Jucker M: Extracellular amyloid formation and associated pathology in neural grafts. Nat Neurosci 2003, 6:370–377
51. Calhoun ME, Burgermeister P, Phinney AL, Stalder M, Tolnay M, Wiederhold KH, Abramowski D, Sturchler-Pierrat C, Sommer B, Staufenbiel M, Jucker M: Neuronal overexpression of mutant amyloid precursor protein results in prominent deposition of cerebrovascular amyloid. Proc Natl Acad Sci USA 1999, 96:14088–14093
52. Shibata M, Yamada S, Kumar SR, Calero M, Bading J, Frangione B, Holtzman DM, Miller CA, Strickland DK, Ghiso J, Zlokovic BV: Clearance of Alzheimer's amyloid-ss(1-40) peptide from brain by LDL receptor-related protein-1 at the blood-brain barrier. J Clin Invest 2000, 106:1489–1499
53. Zlokovic BV: Clearing amyloid through the blood-brain barrier. J Neurochem 2004, 89:807–811
54. Weller RO, Massey A, Newman TA, Hutchings M, Kuo YM, Roher AE: Cerebral amyloid angiopathy: amyloid beta accumulates in putative interstitial fluid drainage pathways in Alzheimer's disease. Am J Pathol 1998, 153:725–733
55. Deane R, Du YS, Submamaryan RK, Larue B, Jovanovic S, Hogg E, Welch D, Manness L, Lin C, Yu J, Zhu H, Ghiso J, Frangione B, Stern A, Schmidt AM, Armstrong DL, Arnold B, Liliensiek B, Nawroth P, Hofman F, Kindy M, Stern D, Zlokovic B: RAGE mediates amyloid-beta peptide transport across the blood-brain barrier and accumulation in brain. Nat Med 2003, 9:907–913

56. Van Dorpe J, Smeijers L, Dewachter I, Nuyens D, Spittaels K, Van Den HC, Mercken M, Moechars D, Laenen I, Kuiperi C, Bruynseels K, Tesseur I, Loos R, Vanderstichele H, Checler F, Sciot R, Van Leuven F: Prominent cerebral amyloid angiopathy in transgenic mice overexpressing the London mutant of human APP in neurons. Am J Pathol 2000, 157:1283–1298
57. Frackowiak J, Miller DL, Potempska A, Sukontasup T, Mazur-Kolecka B: Secretion and accumulation of A beta by brain vascular smooth muscle cells from A beta PP-Swedish transgenic mice. J Neuropathol Exp Neurol 2003, 62:685–696
58. Deane R, Wu ZH, Sagare A, Davis J, Yan SD, Hamm K, Xu F, Parisi M, Larue B, Hu HW, Spijkers P, Guo H, Song XM, Lenting PJ, Van Nostrand WE, Zlokovic BV: LRP/amyloid beta-peptide interaction mediates differential brain efflux of A beta isoforms. Neuron 2004, 43:333–344
59. Collins SR, Douglass A, Vale RD, Weissman JS: Mechanism of prion propagation: amyloid growth occurs by monomer addition. PLOS Biol 2004, 2:E321
60. Iwata N, Tsubuki S, Takaki Y, Watanabe K, Sekiguchi M, Hosoki E, Kawashima-Morishima M, Lee HJ, Hama E, Sekine-Aizawa Y, Saido TC: Identification of the major Abeta1-42-degrading catabolic pathway in brain parenchyma: suppression leads to biochemical and pathological deposition. Nat Med 2000, 6:143–150
61. DeMattos RB, Bales KR, Cummins DJ, Paul SM, Holtzman DM: Brain to plasma amyloid-beta efflux: a measure of brain amyloid burden in a mouse model of Alzheimer's disease. Science 2002, 295:2264–2267
62. Matsuoka Y, Saito M, LaFrancois J, Saito M, Gaynor K, Olm V, Wang LL, Casey E, Lu YF, Shiratori C, Lemere C, Duff K: Novel therapeutic approach for the treatment of Alzheimer's disease by peripheral administration of agents with an affinity to beta-amyloid. J Neurosci 2003, 23:29–33